Two-Photon Diffraction and Quantum Lithography

Milena D'Angelo, Maria V. Chekhova,* and Yanhua Shih
Department of Physics, University of Maryland, Baltimore County, Baltimore, Maryland 21250
(Received 2 February 2001; published 14 June 2001)

We report a proof-of-principle experimental demonstration of quantum lithography. Utilizing the entangled nature of a two-photon state, the experimental results have beaten the classical diffraction limit by a factor of 2. This is a quantum mechanical two-photon phenomenon but not a violation of the uncertainty principle.

DOI: 10.1103/PhysRevLett.87.013602 PACS numbers: 42.50.Dv, 03.65.Ta, 42.25.Fx, 42.82.Cr

Classical optical lithography technology is facing its limit due to the diffraction effect of light. However, this classical limit can be surpassed, surprisingly, by utilizing the quantum nature of entangled multiphoton states [1]. In an idealized experimental situation, the minimum width of the entangled N-photon diffraction pattern can be N times narrower than the width of the corresponding classical diffraction pattern. The working principle of the effect has been discussed theoretically by Boto *et al.* [2], and by Scully from a different approach [3]. In particular, one can consider two-photon entangled states. For a two-particle maximally entangled EPR state, the value of an observable for neither single subsystem is determined. However, if one subsystem is measured to be at a certain value for an observable, the value of that observable for the other subsystem is determined with certainty [1]. Because of this peculiar quantum nature, the two-photon diffraction pattern can be narrower, under certain conditions, than the one given by the classical limit. This effect has been experimentally observed by Kim and Shih [4].

We wish to report a proof-of-principle quantum lithography experiment in this Letter. By using entangled photon pairs in Young's two-slit experiment, we found that *under certain experimental conditions,* the two-photon interference-diffraction pattern has a spatial interference modulation period smaller and a diffraction pattern width narrower, by a factor of 2, than in the classical case.

One of the principles of geometrical optics is that "light propagates in a straight line." If this were always true, one could obtain the image of a physical object, for example, a physical slit, with an unlimited small size by applying a perfect lens system. Unfortunately, light is also a wave. The minimum size of the image one can make is determined by the wave property of light: diffraction. The physics is very simple: according to the Huygens-Fresnel principle, each point on the primary wave front serves as the source of spherical secondary amplitudes (wavelets) and advances with the same speed and frequency as those of the primary wave. The wavelets from a physical slit will meet at any point in space with different phases. The superposition of the wavelets will determine the size of the image. The intensity distribution of light can be calculated by considering an integral of the wavelets coming from the physical object.

Consider a classical one-dimensional optical diffraction by a single slit. A well-collimated laser beam passes the slit and then its intensity distribution is analyzed in the Fourier transform plane (or in the far-field zone). This distribution, which is the diffraction pattern of a single slit, is well known as $\mathrm{sinc}^2(\beta)$, where $\mathrm{sinc}(\beta) = \sin(\beta)/\beta$, the parameter $\beta = (\pi a/\lambda)\sin\theta \simeq (\pi a/\lambda)\theta$, a is the width of the slit, and θ is the scattering angle [5]. When β reaches π, the superposition of the wavelets results in a minimum intensity. The $\mathrm{sinc}^2(\beta)$ pattern determines the minimum width one can obtain. Usually, this minimum width is called the "diffraction limit."

To surpass the diffraction limit, our scheme is to utilize the entangled nature of an N-particle system. To understand the physics of this scheme, consider the *gedanken experiment* illustrated in Fig. 1(a). An entangled photon pair can be generated anywhere in region V; however, photons belonging to the same pair can only propagate (1) *oppositely* and (2) *almost horizontally* (quantitative discussion

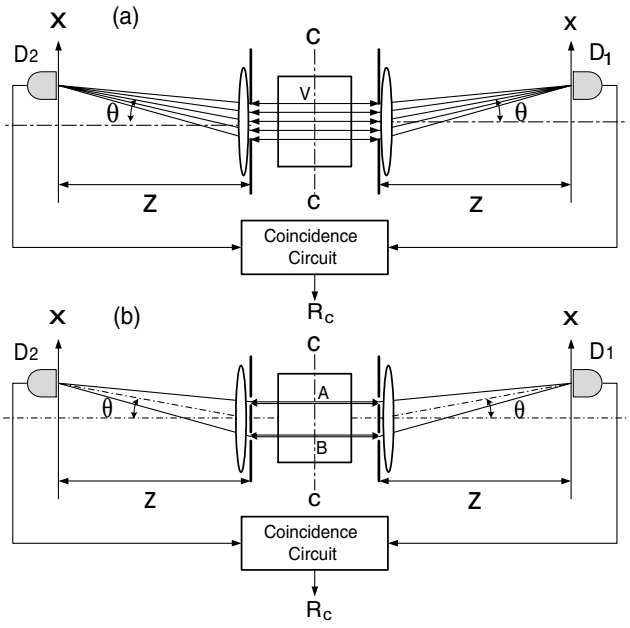

FIG. 1. Schematic of a two-photon diffraction-interference *gedanken experiment.* The right and left sides of the picture represent signal and idler photons of an entangled pair. Detectors D_1, D_2 perform the joint detection (coincidence) measurement.

will be given later) as indicated in the figure. Two slits are placed symmetrically on the left and right sides of the entangled photon source. A photon counting detector is placed into the far-field zone (or the Fourier transform plane, if lenses are placed following the slits) on each side, and the coincidences between the "clicks" of both detectors are registered. The two detectors are scanning symmetrically, i.e., for each coincidence measurement, both detectors have equal x coordinates. A two-photon joint detection is the result of the superposition of the two-photon amplitudes, which are indicated in the figure by straight horizontal lines [6]. To calculate two-photon diffraction, we need to "superpose" all possible two-photon amplitudes. Different from the classical case, a double integral is necessary involving the two slits and the two-photon amplitudes (parallel lines in Fig. 1). The two-photon counterpart of the classical intensity, the joint detection counting rate, is now $\mathrm{sinc}^2(2\beta)$, which gives a distribution narrower than the classical pattern by a factor of 2. Now if we "fold" the symmetrical left and right sides of the experimental setup together and replace the two independent detectors with a film that is sensitive only to two-photon light (two-photon transition material), then, in principle, we have two-photon lithography.

If one replaces the single slit in the above setup with a double slit, Fig. 1(b), it is interesting to see that under the half-width diffraction pattern, the double-slit two-photon spatial interference pattern has a higher modulation frequency, as if the wavelength of the light were reduced to one-half. To observe the two-photon interference, one has to "erase" the first-order interference by reinforcing an experimental condition: $\delta\theta > \lambda/b$, where $\delta\theta$ is the divergence of the light, b is the distance between the two slits, and λ is the wavelength.

The heart of this *gedanken experiment* is a special two-photon source: the pair has to be generated in such a desired entangled way as described above. We have found and demonstrated that, *under certain conditions,* the two-photon state generated via spontaneous parametric down-conversion (SPDC) satisfies the above requirements. The working principle, as well as the report of a real experiment, will be given below.

The schematic setup of the experiment is illustrated in Fig. 2. It is basically the "folded" version of the double-slit interference-diffraction experiment shown in Fig. 1(b). The 458 nm line of an argon ion laser is used to pump a $5mm$ BBO ($\beta - \mathrm{BaB_2O_4}$) crystal, which is cut for degenerate collinear type-II phase matching [7,8] to produce pairs of orthogonally polarized signal (e ray of the BBO) and idler (o ray of the BBO) photons. Each pair emerges from the crystal collinearly, with $\omega_s \simeq \omega_i \simeq \omega_p/2$, where ω_j $(j = s, i, p)$ are the frequencies of the signal, idler, and pump, respectively. The pump is then separated from the signal-idler pair by a mirror M, which is coated with reflectivity $R \simeq 1$ for the pump and transmissivity $T \simeq 1$ for the signal idler.

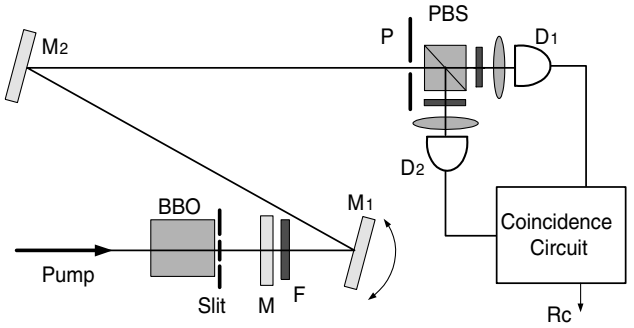

FIG. 2. Schematic of the experimental setup. Details are given in the text.

For further pump suppression, a cutoff filter F is used. The signal-idler beam passes through a double slit, which is placed close to the output side of the crystal, and is reflected by two mirrors, M_1 and M_2, onto a pinhole P followed by a polarizing beam splitter PBS. The signal and idler photons are separated by PBS and are detected by the photon counting detectors D_1 and D_2, respectively. The output pulses of each detector are sent to a coincidence counting circuit with a 1.8 ns acceptance time window for the signal-idler joint detection. Both detectors are preceded by 10 nm bandwidth spectral filters centered at the degenerate wavelength, 916 nm. The whole block containing the pinhole, PBS, the detectors, and the coincidence circuit can be considered as a two-photon detector. Instead of moving two detectors together as indicated in Fig. 1, we rotate the mirror M_1 to "scan" the spatial interference-diffraction pattern relative to the detectors.

One important point to be emphasized is that the double slit must be placed *as close as possible* to the output surface of the BBO crystal. Only in this case, the observed diffraction pattern can be narrower than in the classical case by a factor of 2; see Eq. (9). Otherwise, it will be close to $\sqrt{2}$ as suggested in Ref. [3].

Figure 3 reports the experimental results. In our experiment, the width of each slit is $a = 0.13$ mm. The distance between the two slits is $b = 0.4$ mm. The distance between the double slit and the pinhole P is 4 m. Figure 3(a) shows the distribution of coincidences versus the rotation angle θ of mirror M_1. The spatial interference period and the first zero of the envelope are measured to be 0.001 and ± 0.003 radians, respectively.

For comparison, we also measured the first-order interference-diffraction pattern of a classical light with 916 nm wavelength by the same double slit in the same experimental setup; see Fig. 3(b). The spatial interference period and the first zero of the envelope are measured to be 0.002 and ± 0.006 radians, respectively.

In both "classical" and "quantum" cases, we obtain similar standard Young's two-slit interference-diffraction patterns, $\mathrm{sinc}^2[(\pi a/\lambda)\theta]\cos^2[(\pi b/\lambda)\theta]$; however, whereas the wavelength for fitting the curve in Fig. 3(b) (classical light) is 916 nm, for the curve in Fig. 3(a) (entangled

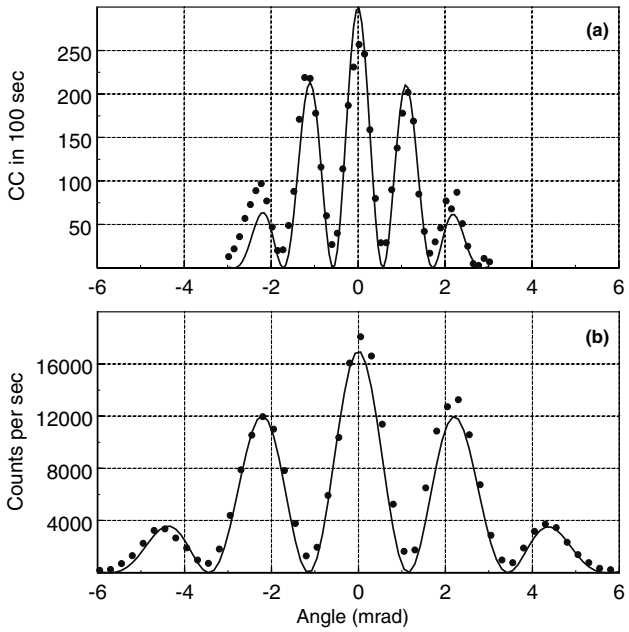

FIG. 3. (a) Experimental measurement of the coincidences for the two-photon double-slit interference-diffraction pattern. (b) Measurement of the interference-diffraction pattern for classical light in the same experimental setup. With respect to the classical case, the two-photon pattern has a faster spatial interference modulation and a narrower diffraction pattern width, by a factor of 2.

two-photon source) it has to be 458 nm. Clearly, the two-photon diffraction "beats" the classical limit by a factor of 2.

To be sure that we observed the effect of the SPDC photon pair with wavelength of 916 nm but not the pump laser beam with wavelength of 458 nm, we remove or rotate the BBO crystal 90° to a non-phase-matching angle and examine the coincidence counting rate. The coincidences remain zero during the 100 sec period, which is the data collection time duration for each of the data points, even in high power operation of the pump laser. Comparing this with the coincidence counting rate obtained with BBO under phase matching, see Fig. 3(a), there is no doubt that the observation is the effect due to the SPDC photon pairs.

To explain the result, we have to take into account the quantum nature of the two-photon state. SPDC is a nonlinear optical process in which pairs of signal-idler photons are generated when a pump laser beam is incident onto an optical nonlinear material [7,8]. Quantum mechanically, the state can be calculated by the first-order perturbation theory [7] and has the form

$$|\Psi\rangle = \sum_{s,i} F(\omega_s, \omega_i, \mathbf{k}_s, \mathbf{k}_i) a_s^\dagger[\omega(\mathbf{k}_s)] a_i^\dagger[\omega(\mathbf{k}_i)] \,|\, 0\rangle, \tag{1}$$

where ω_j, $\mathbf{k}_j$ $(j = s, i, p)$ are the frequencies and wave vectors of the signal (s), idler (i), and pump (p), respectively, $F(\omega_s, \omega_i, \mathbf{k}_s, \mathbf{k}_i)$ is the so-called biphoton amplitude, and $a_s^\dagger$ and $a_i^\dagger$ are creation operators for the signal and idler photons, respectively. The pump frequency ω_p and wave vector $\mathbf{k}_p$ can be considered as constants. The biphoton amplitude contains δ functions of the frequency and wave vector,

$$F(\omega_s, \omega_i, \mathbf{k}_s, \mathbf{k}_i) \propto \delta(\omega_s + \omega_i - \omega_p) \times \delta(\mathbf{k}_s + \mathbf{k}_i - \mathbf{k}_p). \tag{2}$$

The signal or idler photon could be in any mode of the superposition (uncertain); however, due to Eq. (2), if one photon is known to be in a certain mode then the other one is determined with certainty.

The phase-matching conditions resulting from the δ functions in Eq. (2),

$$\omega_s + \omega_i = \omega_p, \qquad \mathbf{k}_s + \mathbf{k}_i = \mathbf{k}_p, \tag{3}$$

play an important role in the experiment. The transverse component of the wave vector phase-matching condition requires that

$$k_s \sin\alpha_s = k_i \sin\alpha_i, \tag{4}$$

where α_s and α_i are the scattering angles inside the crystal. Upon exiting the crystal, Snell's law thus provides

$$\omega_s \sin\beta_s = \omega_i \sin\beta_i, \tag{5}$$

where β_s and β_i are the exit angles of the signal and idler with respect to the $\mathbf{k}_p$ direction. Therefore, in the degenerate case, the signal and idler photons are emitted at equal, yet opposite, angles relative to the pump, and the measurement of the momentum (wave vector) of the signal photon determines the momentum (wave vector) of the idler photon with unit probability and vice versa. In the collinear case, which we use in our experiment, the scattering angles of the signal and idler photons are close to zero and occupy the range $\Delta\theta$, which is determined by the size of both the crystal and the pump beam; see [9].

The coincidence counting rate R_c is given by the probability P_{12} of detecting the signal-idler pair by detectors D_1 and D_2 jointly,

$$\begin{aligned} P_{12} &= \langle\Psi|E_1^{(-)}E_2^{(-)}E_2^{(+)}E_1^{(+)}|\Psi\rangle \\ &= |\langle 0|E_2^{(+)}E_1^{(+)}|\Psi\rangle|^2, \end{aligned} \tag{6}$$

where $|\Psi\rangle$ is the two-photon state of SPDC and E_1, E_2 are fields on the detectors. The effect of two-photon Young's interference can be easily understood if we assume for simplicity that signal and idler photons always go through the same slit and never go through different slits. This approximation holds if the variation of the scattering angle inside the crystal satisfies the condition:

$$\Delta\theta \ll b/D, \tag{7}$$

where D is the distance between the input surface of the SPDC crystal and the double slit. In this case, the state after the double slit can be written as

$$|\Psi\rangle = |0\rangle + \epsilon[a_s^\dagger a_i^\dagger \exp(i\varphi_A) + b_s^\dagger b_i^\dagger \exp(i\varphi_B)]|0\rangle, \tag{8}$$

where $\epsilon \ll 1$ is proportional to the pump field and the nonlinearity of the crystal, φ_A and φ_B are the phases of the

pump field at region A (upper slit) and region B (lower slit), respectively, and $a_j^\dagger$, $b_j^\dagger$ are the photon creation operators for photons passing through the upper slit (A) and the lower slit (B), respectively. In our experiment, the ratio $(b/D)/\Delta\theta \simeq 30$ and Eq. (7) are satisfied well enough. Moreover, even the ratio $(a/D)/\Delta\theta$ is of the order of 10, which satisfies the condition for observing two-photon diffraction:

$$\Delta\theta \ll a/D\,. \tag{9}$$

In Eq. (6), the fields on the detectors are given by

$$\begin{aligned} E_1^{(+)} &= a_s \exp(ikr_{A1}) + b_s \exp(ikr_{B1})\,, \\ E_2^{(+)} &= a_i \exp(ikr_{A2}) + b_i \exp(ikr_{B2})\,, \end{aligned} \tag{10}$$

where r_{Ai} (r_{Bi}) are the optical path lengths from region A (B) to the ith detector. Substituting Eqs. (8) and (10) into Eq. (6), we get

$$\begin{aligned} R_c \propto P_{12} &= \epsilon^2 |\exp(ikr_A + i\varphi_A) + \exp(ikr_B + i\varphi_B)|^2 \\ &\propto 1 + \cos[k(r_A - r_B)], \end{aligned} \tag{11}$$

where we define $r_A \equiv r_{A1} + r_{A2}$ ($r_B \equiv r_{B1} + r_{B2}$). We have assumed $\varphi_A = \varphi_B$ in Eq. (11).

In the far-field zone (or the Fourier transform plane), interference of the two amplitudes from Eq. (8) gives

$$R_c(\theta) \propto \cos^2[(2\pi b/\lambda)\theta]. \tag{12}$$

Equation (12) has the form of a standard Young's two-slit interference pattern, except having the modulation period one-half of the classical case or an equivalent wavelength of $\lambda/2$.

To calculate the diffraction effect of a single slit, we need an integral of the effective two-photon wave function over the slit width. Quite similarly to Eq. (12), it gives

$$R_c(\theta) \propto \mathrm{sinc}^2[(2\pi a/\lambda)\theta]. \tag{13}$$

Equation (13) has the form of a standard single-slit diffraction pattern, except having one-half of the classical pattern width.

The combined interference-diffraction coincidence counting rate for the double-slit case is given by

$$R_c(\theta) \propto \mathrm{sinc}^2[(2\pi a/\lambda)\theta]\cos^2[(2\pi b/\lambda)\theta], \tag{14}$$

which is a product of Eqs. (12) and (13).

The experimental observations have confirmed the above quantum mechanical predictions.

In conclusion, we have demonstrated the possibility of quantum lithography by using an entangled two-photon state generated by a specially designed spontaneous parametric down-conversion. One may not see immediate practical advantages from the above proof-of-principle experimental demonstration. The advantage, however, is in the case of a large number of entangled particle states. Based on our entangled N-photon scheme ($N \geq 3$) [10] one can beat the classical limit by a factor of N and keep the "pump" laser beam wavelength close to one-half that of the entangled photon beam. This is a quantum mechanical N-photon phenomenon but not a violation of the uncertainty principle. There are also other mechanisms of breaking the classical diffraction limit for lithography, for example, near-field scanning optical microscopy [11].

The authors thank Y.-H. Kim, J. P. Dowling, D. V. Strekalov, M. O. Scully and H. S. Pilloff for helpful discussions. This work was supported, in part, by ARDA-NSA, ONR, and NSF. M. V. C. acknowledges the support from the Russian Foundation for Basic Research, Grant No. 99-02-16419.

*Permanent address: Department of Physics, Moscow State University, Moscow, Russia.

[1] A. Einstein, B. Podolsky, and N. Rosen, Phys. Rev. **47**, 777 (1935).
[2] A. N. Boto *et al.,* Phys. Rev. Lett. **85**, 2733 (2000).
[3] M. O. Scully, in *Proceedings of the Conference on Effects of Atomic Coherence and Interference in Quantum Optics, Crested Butte, Colorado, 1993* (IOP, Bristol, 1994); see also U. Rathe and M. O. Scully, Lett. Math. Phys. **34**, 297 (1995).
[4] Y.-H. Kim and Y. H. Shih, Found. Phys. **29**, 1849 (1999).
[5] See classical optics textbooks, for example, E. Hecht, *Optics* (Addison-Wesley, Reading, MA, 1989), 2nd ed.
[6] T. B. Pittman *et al.,* Phys. Rev. A **52**, R3429 (1995); D. V. Strekalov *et al.,* Phys. Rev. Lett. **74**, 3600 (1995).
[7] D. N. Klyshko, *Photons and Nonlinear Optics* (Gordon and Breach Science, New York, 1988).
[8] A. Yariv, *Quantum Electronics* (John Wiley and Sons, New York, 1989).
[9] A. V. Burlakov, M. V. Chekhova, D. N. Klyshko, S. P. Kulik, A. N. Penin, Y. H. Shih, and D. V. Strekalov, Phys. Rev. A **56**, 3214 (1997).
[10] T. E. Keller, M. H. Rubin, Y. H. Shih, and L. A. Wu, Phys. Rev. A **57**, 2076 (1998).
[11] See, for example, C. Fischer, *Scanning Probe Microscopy,* edited by R. Wiesendanger (Springer, New York, 1998), and references cited therein.